Title
SHAPE-RESONANT AND MANY-ELECTRON EFFECTS IN THE S 2P PHOTOIONIZATION SF[SUB]6

Authors
Ferrett, T.A.
Lindle, D.M.
Heimann, P.A.

Publication Date
1988-04-01

LBL-18829
Preprint

Lawrence Berkeley Laboratory
UNIVERSITY OF CALIFORNIA

Materials & Chemical Sciences Division

Submitted to Journal of Chemical Physics

Shape-resonant and Many-electron Effects in the S 2p Photoionization of SF_6

T.A. Ferrett, D.W. Lindle, P.A. Heimann, M.N. Piancastelli, P.H. Kobrin, H.G. Kerkhoff, U. Becker, W.D. Brewer, and D.A. Shirley

April 1988

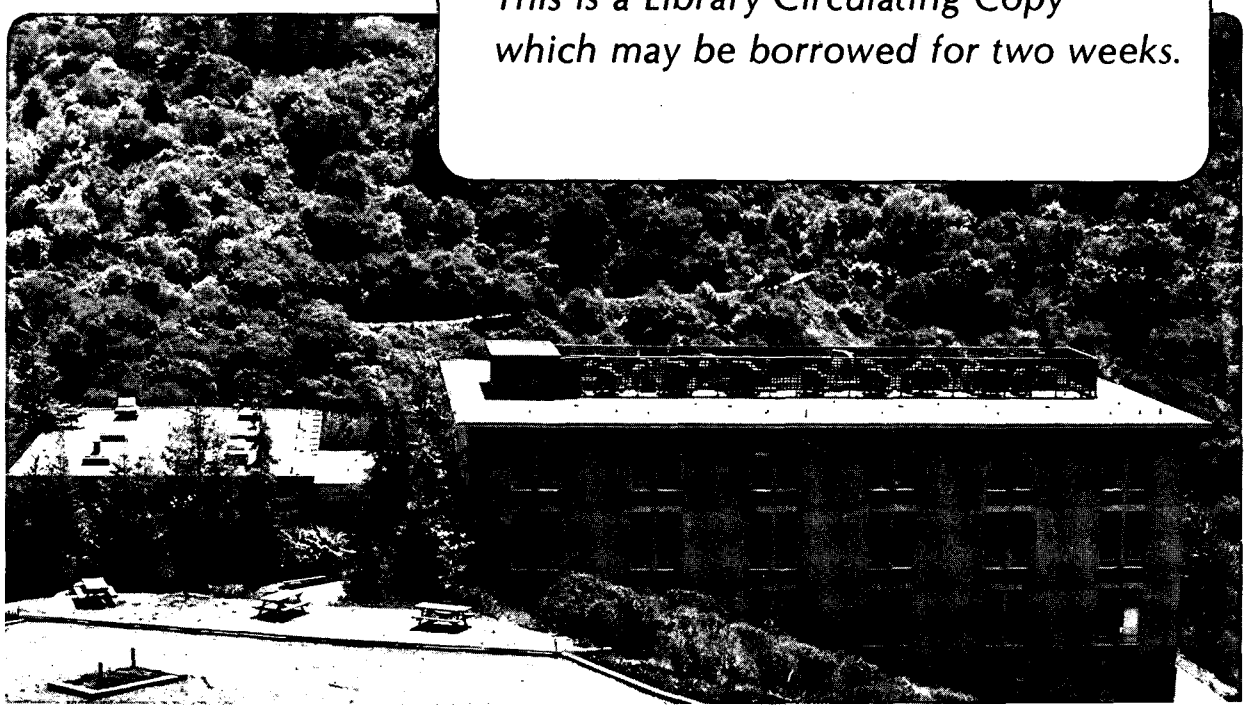

Prepared for the U.S. Department of Energy under Contract Number DE-AC03-76SF00098.

DISCLAIMER

Shape-resonant and Many-electron Effects in the S 2p Photoionization of SF_6

T.A. Ferrett, D.W. Lindle, P.A. Heimann, M.N. Piancastelli, P.H. Kobrin, H.G. Kerkhoff, U. Becker, W.D. Brewer, and D.A. Shirley

Department of Chemistry, University of California
and
Materials and Chemical Sciences Division
Lawrence Berkeley Laboratory, 1 Cyclotron Road
Berkeley, California 94720

This work was supported by the U. S. Department of Energy under Contract No. DE-AC-3-76SF00098.

Shape-resonant and Many-electron Effects in the S 2p Photoionization of SF_6

T.A. Ferrett,* D.W. Lindle,* P.A. Heimann,† M.N. Piancastelli,¶ P.H. Kobrin,§ H.G. Kerkhoff,[a] U. Becker,[a] W.D. Brewer,[b] and D.A. Shirley

Department of Chemistry, University of California
and
Materials and Chemical Sciences Division
Lawrence Berkeley Laboratory, 1 Cyclotron Road
Berkeley, California 94720

Abstract

The core-level photoexcitation and photoionization of SF_6 were studied in the vicinity of the resonances below and above the S 2p threshold. The decay channels of the S 2p$\rightarrow 6a_{1g}$ discrete excitation were characterized, with decay leading mostly to valence-shell satellites. The S 2p continuum data show an oscillatory asymmetry parameter β(S 2p) near threshold that is virtually identical to β(Si 2p) in SiF_4. It also resembles - but differs from - theoretical curves for β(S 2p) in atomic sulfur and in SF_6. Data at the feature assigned as an e_g shape resonance indicate strong multi-electron properties for this state, because a resonance in the S 2p satellite is observed at the same photon energy as the main-line resonance. We propose a unified model which generally includes configuration interaction both in the continuum-state

manifold and between discrete doubly-excited states and the continua, to explain this unexpected satellite behavior. Finally, the $S(L_{2,3}VV)$ Auger electron asymmetry parameter shows no significant deviation from zero near the t_{2g} and e_g shape resonances.

*Present address: National Bureau of Standards, Gaithersburg, MD, 20899.
†Technische Universität München, Physik-Department E20, 8046 Garching b. Munchen, West Germany.
¶Permanent address: Department of Chemistry, University of Rome "La Sapienza", 00100 Rome, Italy.
§Present address: Rockwell International, P.O. Box 1085, Thousand Oaks, CA, 91360.
[a]Permanent address: Technische Universität Berlin, Institut für Strahlungs und Kernphysik, Sekr. PN 3-2, Hardenbergstr. 36, D-1000 Berlin 12, West Germany.
[b]Permanent address: Institut für Atom- und Festkörperphysik, Freie Universität Berlin, Arnimalee 14, 1000 Berlin 33, West Germany.

I. Introduction

The distinctive structures in the photoabsorption spectra around the K and L thresholds of highly symmetric molecules have received much attention in recent years.[1-10] For example, spectra near the sulfur and silicon 2p edges in SF_6, SiF_4, and SO_2 are each characterized by two resonances in the L continua, as shown in Fig. 1.[3] The S 2p absorption spectrum for SF_6 exhibits the narrowest (2-4 eV) and most intense continuum resonances, relative to the discrete resonant intensity, in this series.[3] The resonances in these absorption spectra have been interpreted within a potential-barrier model, with the strongest effects being present in high-symmetry molecules containing the most electronegative ligands.[3,5,8,10] Both of these factors tend to enhance the spatial extent and height of the barrier.

The potential-barrier or shape-resonance model that has been widely used in the literature to interpret the molecular absorption spectra is described within a one-electron framework. In this picture, an emerging photoelectron experiences a centrifugal barrier in the molecular potential through which it can tunnel and propagate in the continuum, with an enhanced photoionization cross section and a perturbed angular distribution, at a particular kinetic energy. In this description, a shape resonance is strictly a single-channel final-state effect. Shape resonances have been treated as such[10-13] in all but two theoretical calculations[14] to date. Because of its final-state nature, a shape resonance is usually interpreted as

decaying into only one final-state configuration (e.g., only the 2p main-line photoemission intensity should be enhanced at a shape resonance above the $L_{2,3}$ edge). The trapped photoelectron can also be thought of as forming a quasi-bound state associated with an unoccupied molecular orbital in the continuum.[2,4-5,12] The relation of this model to the potential-barrier approach has been discussed.[7]

Though numerous photoabsorption measurements have been made near the K and L edges in small molecules,[1-3,15] only a handful of photoemission experiments have been performed to study the decay properties of core-level shape resonances.[16-20] Photoionization experiments on the C and N 1s levels in CO, CO_2,[16] N_2, and NO[17] and on the Si 2p level of SiF_4[19] indicate that the one-electron potential-barrier model is adequate to explain the observed decay to single-ion final states with a core hole (photoemission main lines). However, the continuum resonances in these molecules are not very intense (except for SiF_4), and they have widths on the order of 5-10 eV,[16,17] in contrast to the especially narrow and intense continuum resonances in the S 2p photoabsorption spectrum of SF_6.[3]

To understand the unusual aspects of the resonances in SF_6, we have investigated the resonance behavior of the S 2p main line and its correlation satellites using angle-resolved time-of-flight (TOF) photoelectron spectroscopy. We have measured the photoionization partial cross sections and angular-distribution asymmetry parameters for the S 2p and valence photoelectrons and the $S(L_{2,3}VV)$ Auger electrons in the photon-energy range $h\nu$ = 150-260 eV. Figure 2

illustrates a molecular orbital diagram for SF_6, indicating the transitions studied in this work. Below the S 2p ($2t_{1u}$) core-level threshold, we have attempted to characterize qualitatively the decay of the $2t_{1u} \rightarrow 6a_{1g}$ discrete resonance by measuring the cross sections and asymmetry parameters for the important photoemission decay channels to SF_6^+. Above the S 2p threshold, we have observed several correlation satellites of the S 2p main line, one of which participates in the decay of the continuum resonance at 196.5 eV photon energy, which has been assigned as the e_g shape resonance. The cross section and asymmetry parameter for this S 2p satellite over the resonance region also are reported.

In the vicinity of the S 2p edge, our observation of a S 2p satellite enhanced at the same photon energy as the S 2p main line at the so-called e_g shape resonance (196.5 eV) forces us to consider the many-electron nature of this continuum resonance. Because of these unusual decay properties, we will refer to the resonance at 196.5 eV as the "e_g" resonance to indicate uncertainty in its historical assignment. The naive shape resonance picture of a "pure" one-electron final-state effect is clearly inadequate because the S 2p main-line and satellite photoelectrons are at different kinetic energies at the "e_g" resonance. Recent photoemission studies of the valence shells of SF_6 also indicated that something beyond a one-electron description is needed to explain the valence t_{2g} resonance, which appears to exhibit coupling to neighboring valence photoemission channels at 23 eV photon energy.[21,22] In that case, continuum-continuum coupling was proposed to explain the participation

of the final states of even parity in the t_{2g} shape resonance.[21] However, the absence of the e_g shape resonance in the valence shells of SF_6 is especially surprising because in our present understanding it seems to play an important and unusual role above the S 2p edge.

On the theoretical side, K-matrix calculations have established a precedent for continuum-continuum coupling to neighboring channels for a valence shape resonance in N_2,[14] where the angular distribution of the $2\sigma_u$ photoelectrons is affected at the σ_u shape resonance.[23-24] Continuum-continuum interchannel coupling as proposed in N_2 (Ref. 14) may cause the S 2p main-line and satellite continuum states to share in the "e_g" resonance intensity. Nonresonant interchannel coupling effects are typically small;[25] however, the production of a quasibound shape-resonant continuum state provides a situation where the coupling may be enhanced because of the larger continuum-state amplitude within the molecule.[14]

We propose a more general approach to explain the "e_g" resonance decay, which includes continuum-continuum coupling as well as configurational mixing of doubly excited states. Electron correlation in this model allows for continuum coupling and the possible energy degeneracy of discrete doubly excited states with the "e_g" resonance; it adequately describes the observed decay to both main-line and satellite channels.

The experimental procedures are described in Sec. II. The discrete S 2p $(2t_{1u})\rightarrow 6a_{1g}$ resonance data near 173 eV photon energy are discussed in Sec. III. The extended-energy-range (185-260 eV) results for the S 2p main line, satellites, and $S(L_{2,3}VV)$ Auger

electrons appear in Sec. IV, with emphasis on the behavior at the "e_g" shape resonance (196.5 eV). Section V concludes the interpretation of the SF_6 data.

II. Experimental

Synchrotron radiation from Beam line III-1, equipped with a "grasshopper" monochromator, at the Stanford Synchrotron Radiation Laboratory (SSRL) was used to photoionize an effusive jet of gas. Photoelectrons and Auger electrons were detected simultaneously at 0° and 54.7° relative to the photon polarization direction using the double-angle time-of-flight (TOF) technique.[26-28] These angles were chosen to facilitate the simultaneous determination of the partial cross section $\sigma(\varepsilon)$ and the angular distribution asymmetry parameter $\beta(\varepsilon)$, using Yang's theorem.[29] Calibration of the TOF analyzers was accomplished with the 2s and 2p levels of Ne^+ (Ref. 30) and the 3d level of Kr^+ (Ref. 31), for which $\sigma(\varepsilon)$ and $\beta(\varepsilon)$ are known. Here ε is the electron kinetic energy. We estimate that systematic errors (not represented by the statistical error bars in our plots) are less than 10 percent for $\sigma(\varepsilon)$ and ±0.10 for $\beta(\varepsilon)$.

A 1000-Å-thick vitreous carbon window separated the sample-chamber pressure (10^{-4} torr) from the monochromator vacuum (10^{-10} torr). Photoelectron spectra were taken in the photon-energy range $160 \leq h\nu \leq 250$ eV using a 1200 line/mm holographically ruled grating. The monochromator resolution varied from 1.3 to 3.3 eV over this range. Energy calibration of the monochromator to within 0.5 eV

was based on the positions of the resonances in the SF_6 total cross section at 173 eV ($2t_{1u} \rightarrow 6a_{1g}$), 184 eV ($2t_{1u} \rightarrow t_{2g}$), and 196.5 eV ($2t_{1u} \rightarrow e_g$).[5]

The SF_6 relative sample pressure was monitored with a capacitance manometer and the photon intensity was monitored by a sodium salicylate scintillator with an optical photomultiplier tube (RCA 8850). Corrections have been made in the measured cross sections for the varying response of sodium salicylate in our system over the photon-energy range of this study.[32]

A S 2p time-of-flight spectrum taken for 300 sec at $\theta = 54.7°$ and at $h\nu = 196.5$ eV is presented in Fig. 3, showing the S 2p main-line (binding energy = 181 eV)[33] and satellite peaks, the $S(L_{2,3}VV)$ Auger peaks, and the inner- and outer-valence peaks at high kinetic energy. Typical off-resonance count rates were 50 counts/sec for the S 2p level, 5-10 counts/sec for the S 2p satellites, and 300 counts/sec for the total valence intensity.

The major discrete and continuum resonance effects near the S 2p edge can be seen in Fig. 4. The experimental data below the S 2p threshold represent the total inner- and outer-valence intensity, and above threshold, the sum of the valence and $S(L_{2,3}VV)$ Auger intensity. For comparison, the photoabsorption curve[1] is plotted, along with our total measured valence main-line cross section.

III. The S 2p ($2t_{1u}$)-->$6a_{1g}$ Resonance

Recent work on the decay properties of discrete core-level excitations in atoms and small molecules has provided a framework in which to describe subsequent decay to singly-charged ionic final states.[34-39] These final states often appear as "spectator" satellite peaks in the photoelectron spectrum; they correspond to correlation satellite states of the ion possessing two holes in normally filled orbitals and an additional electron in the orbital initially reached by the excitation process in the neutral. During decay to these final states, the excited electron may be regarded as a "spectator" to an Auger-like process in which the core hole is filled by one electron and another is ejected.

However, not all decay channels leave the initially excited electron as a noninteracting spectator. The direct involvement of this electron in the decay can produce the same "main line" states reached by photoemission; i.e., final states corresponding to singly-charged ions with one hole. Thus, "nonspectator" satellites can be produced in the decay following discrete core-level excitation when the excited electron is left in an orbital other than the one to which it is initially excited. The fractional extent to which the excited electron participates has been found to account for 5-25 percent of the resonance intensity in the few molecular systems studied to date.[37]

The relative amounts of spectator and participatory decay have been found to vary at the intense $1s \rightarrow \pi^*$ resonances below the C, O, and N K edges in CO and N_2.[37] The variations are related to the coupling of the initially excited electron to the rest of the ion in the decay process. To a first approximation, participatory decay is expected to be favored when the initially excited π^* electron is localized on the atom with the core hole.[37]

Below the S 2p edge in SF_6, the $(2t_{1u})^{-1}6a_{1g}$ neutral excited state can autoionize to outer- or inner-valence main-line photoemission final states, to valence shake-up satellites (participatory decay), and to "spectator" satellites. These states are illustrated in Fig. 5 in the binding-energy spectra taken on (172.9 eV) and off (176.1 eV) resonance. Qualitatively, the unresolved outer-valence peaks with binding energies between 15 and 27 eV show little resonance enhancement, in contrast to the large electron intensity increase in the binding-energy range 35-60 eV. Included in the region labelled "inner" valence are the unresolved outer- and inner-valence satellites, plus the inner-valence main-line peaks ($2e_g$, $3t_{1u}$, and $4a_{1g}$).[40] The total valence intensity (main lines and satellites) over the $6a_{1g}$ resonance was plotted as a dashed curve in Fig. 4.

Though it is not possible in the TOF photoelectron spectrum to resolve the outer-valence satellites from the inner-valence main lines, peak shapes differ on and off resonance in the binding-energy region of 35-45 eV. On resonance, there are greater contributions at binding energy ~35 eV, indicating some enhancement of outer-valence

satellites. This result has been confirmed qualitatively by electron energy-loss measurements at the S 2p-->$6a_{1g}$ resonance.[41] In addition, there is a resonantly enhanced peak at 55 eV binding energy, corresponding energetically to an inner-valence satellite(s). Thus, we have direct spectroscopic evidence for autoionization decay to satellite channels, although we cannot assess the importance of these channels quantitatively relative to inner-valence main-line decay. However, we observe that decay to outer-valence main lines is not large, accounting for less than 7 percent of the total resonant enhancement of single-ion decay channels.

To document the dominant decay into SF_6^+ final states with binding energies $\geq$35 eV further, the partial cross-section data for the observed outer- and "inner"-valence peaks are shown in Fig. 6, along with the "inner"-valence asymmetry parameter. The "inner"-valence peak integration included the binding-energy range 30 to 100 eV.[42] This energy range carries most of the resonant intensity, in contrast to the small effect on the outer-valence levels. Consistent with this, the outer-valence β is relatively constant over the resonance at a value of 1.36(7), while the "inner"-valence β decreases from an off-resonant value above 1.0 down to 0.3 on resonance.

We conclude that valence satellites are important decay channels for the S 2p-->$6a_{1g}$ resonance, with the prospect that most of the satellites are probably spectator in nature (containing a $6a_{1g}$ electron), though higher (kinetic-energy) resolution studies are needed to confirm this. The amount of enhancement of the

inner-valence main lines ($2e_g$, $3t_{1u}$, and $4a_{1g}$) is not clear because these photoemission peaks are unresolved from the outer-valence satellites. In terms of the $2p^{-1}6a_{1g}$ excited-state localization, the 2p hole is well-localized on the sulfur atom where the $6a_{1g}$ orbital has significant electron density. Thus, some participation of the $6a_{1g}$ electron in the decay to SF_6^+ seems reasonable, explaining the small effect observed in the outer-valence cross section.

Finally, the added complication of many-electron correlations in the inner-valence region should be considered because this produces many overlapping peaks in the photoelectron spectrum, each representing possibly more than one ionic configuration.[43] For example, in the molecules H_2O (Ref. 33, 44) and especially H_2S (Ref. 45), the nonresonant inner-valence spectra are more complex than the one-electron molecular-orbital picture would dictate. Thus, progress in understanding the extent of the many-electron interactions in the inner-valence orbitals is necessary before a more complete picture of the resonant decay to these states can be acquired.

IV. Above the S 2p Main-Line and Satellite Thresholds

The extended energy-range behavior of the S 2p main line (average binding energy of 181 eV)[33] is depicted in Fig. 7. The "e_g" shape resonance is evident in the S 2p cross section at 196.5 eV, and the S 2p β undergoes an oscillation in the vicinity of this resonance. The broader weak feature at ~205 eV in the absorption data (Fig. 4)

may also be present in the S 2p partial-cross-section data. The MSM-Xα S 2p (Ref. 8) and the experimental SiF_4 Si 2p (Ref. 46) asymmetry parameters are plotted for comparison, along with the atomic Hartree-Slater calculations of β(2p) for sulfur.[47] Although we were not able to extend our S 2p measurements down in energy to the t_{2g} shape resonance at 184 eV photon energy (except for one point at 185.7 eV), we note that no enhancement of the valence main lines was observed at the t_{2g} resonance (see dashed curve, Fig. 4). Thus, the following discussion will focus on the observation of S 2p satellites, and the S 2p main-line and satellite behavior near the "e_g" resonance.

Several S 2p correlation satellites were visible in the photoemission spectra, with binding energies of 189(1), 194(1), and 205(2) eV. The corresponding excitation energies above the S(2p) threshold are 8(1), 13(1), and 24(2) eV. The satellites were easily distinguished only at low kinetic energies for each satellite; thus, we show only the resonant satellite [binding energy 189(1) eV] in Fig. 3. We have used the recently proposed valence ordering[21] confirmed by many-body theoretical calculations[48] to estimate the energies of the configurations responsible for the observed satellites. Also utilizing the $4t_{1u} \rightarrow 6a_{1g}$ transition energy of 17 eV in the neutral, we find that the most likely configuration for the lowest-binding-energy satellite is $2p^{-1}1t_{1g}^{-1}6a_{1g}$, which corresponds to an excitation from the highest-occupied ($1t_{1g}$) to the lowest-unoccupied ($6a_{1g}$) molecular orbital. We cannot assign the remaining satellite peaks with certainty (with excitation energies of

13 and 24 eV), but there are several possible configurations in these energy ranges. The likely possibilities are:

$2p^{-1}1t_{2g}^{-1}6a_{1g}$
$2p^{-1}3e_g^{-1}6a_{1g}$
$2p^{-1}(5t_{1u}$ or $1t_{2u})^{-1}6t_{1u}$ } binding energy 194(1) eV

$2p^{-1}4t_{1u}^{-1}6t_{1u}$
$2p^{-1}5a_{1g}^{-1}6a_{1g}$ } binding energy 204(2) eV

The rest of this section will address the results obtained at the t_{2g} and "e_g" continuum resonances, with emphasis on the "e_g" resonance (196.5 eV). Section A includes presentation of the cross-section and asymmetry-parameter data for the S 2p main-line and the 189 eV satellite peaks and for the $S(L_{2,3}VV)$ Auger peak. In Sec. B, we interpret the unusual observation of coupling to other channels at the "e_g" shape resonance, and discuss the possible explanations for this behavior.

A. Photoelectron and Auger Electron Results

The shape of the S 2p cross section and β over the "e_g" resonance appears in Fig. 7, and over a smaller energy range in Fig. 8. The S 2p satellite (binding energy of 189 eV) cross section and β are plotted in Fig. 8 with the main-line results, shown for direct comparison. We observe a large cross-section enhancement of both the S 2p main line and the 189 eV satellite at the same photon

energy. The main-line and satellite asymmetry parameters (Fig. 8) also correlate well as a function of photon energy in the resonance region. This is the first observation of a molecular correlation satellite with enhanced intensity at a feature assigned as a shape resonance.

The TOF spectrum in Fig. 3 taken on the "e_g" resonance illustrates the large satellite intensity, which is about 15 percent that of the main line off resonance, increasing to ~30 percent on resonance. The intensity of the 189(1) eV satellite could be monitored only up to about 200 eV photon energy, above which it was unresolved from the 194(1) eV satellite. Having observed decay into a channel other than the S 2p main line at the "e_g" resonance, we also checked the total valence intensity over the "e_g" resonance region. No measurable enhancement was observed, as seen in the valence cross section shown in Fig. 4 (dashed curve).

The effect in the S 2p β near the "e_g" resonance is dramatic (see Fig. 7), and is partially reproduced by the MSM-Xα calculation[8] when the theory curve is shifted to the experimental resonance energy (i.e., theory shifted to lower energy by 1.8 eV). The width of the resonance is too narrow in the calculation, which is expected because vibrational,[49] orbital-relaxation,[8,50] and intrachannel-coupling effects[51] (all of which tend to broaden the theoretical resonant profiles) have not been included.

It is relevant to consider to what extent the observed effect in β(S 2p) is correlated with the "e_g" resonance rather than just being the natural energy dependence of the angular distribution. It has

been observed experimentally[16,46] and theoretically[8,52] that an increase in the cross section at a core-level molecular shape resonance is generally accompanied by a minimum in β (sometimes offset slightly in energy) for the affected continuum channel.

To assess whether the S 2p β effect is induced primarily by the resonance, we first examine the atomic behavior for a S 2p orbital. The shape of the atomic sulfur β(2p) in Fig. 7 within 30 eV of threshold is the result of the changing Coulomb phase-shift differences between the l+1 and l-1 transitions.[47] The atomic curve has very roughly the same shape as the experimental results for SF_6, with a minimum in β within 15 eV of threshold. However, the atomic curve falls at significantly higher values relative to the experimental SF_6 S 2p asymmetry parameter. Also, the minimum in β(S 2p, SF_6) is more pronounced and occurs over a narrower energy range compared to the atomic β(2p), suggesting an effect due to the molecular resonance.

Secondly, we compare our β(S 2p) curve to β(Si 2p) of SiF_4 in Fig. 7.[46] Within experimental error, the two sets of data are identical as a function of kinetic energy except for a possible small difference in the asymptotic value at high energy. This result is surprising if one believes that the pronounced minima in β are indicative of the resonances in the two molecules (see Fig. 1), which occur at different kinetic energies (3 and 15.5 eV for SF_6; 5.5 and 21.5 eV for SiF_4).[1,53] Furthermore, the decay characteristics of the second resonance for each molecule are markedly different. The SF_6 continuum "e_g" resonance decays to the S 2p main line and to a

S 2p shake-up satellite; in contrast, the broad (~10-15 eV) SiF_4 t_2 shape resonance (21.5 eV kinetic energy) seen in Fig. 1 decays only to the Si 2p main line,[19] thus apparently fitting the one-electron shape-resonance model.

In addition, the Si 2p β curve for $Si(CH_3)_4$, which has been compared previously with SiF_4,[46] has a similar shape but a higher value of β between 5 and 15 eV kinetic energy, relative to SiF_4. This difference has been attributed in part to the different electron densities in the two Si-containing molecules.[46] We also note that the Si 2p cross section in $Si(CH_3)_4$ is different as a function of kinetic energy from both SiF_4 and SF_6, with a series of resonances very near threshold and one broad (~10 eV FWHM) continuum resonance at about 18 eV kinetic energy.[15,20]

The variation in the energies of the continuum resonances in these molecules, coupled with the observation of different decay patterns for the resonances in SiF_4 and SF_6 and the known atomic behavior, strongly suggest that the overall shape of β(S 2p) may have origins in atomic effects as well as shape-resonance effects in these S- and Si-containing molecules. In fact, MSM-Xα asymmetry-parameter results on the Si 2p level in SiF_4 are qualitatively very similar to the atomic Si 2p Hartree-Slater results.[46] Photoemission measurements and calculations on the Si and S 2p levels in molecules which do not exhibit pronounced continuum resonances would help to identify the nonresonant "molecular" behavior of the β parameter at low kinetic energy.

In addition to the effect on the photoelectron asymmetry parameter, the angular distribution of Auger electrons may become anisotropic in the vicinity of a shape resonance. Theoretically, the Auger electron angular distribution (β_{Auger}) has been related to the asymmetry in the molecular orientation of the ion (β_m) as:[54]

$$\beta_{Auger} = c\,\beta_m, \qquad (1)$$

where c is a constant characteristic of a single Auger decay channel. The possibility for ion orientation at a shape resonance may induce an anisotropy in the Auger electron emission, weighted by the factor c. However, there are no known examples of detectable changes in β_{Auger} at a continuum molecular shape resonance, although KVV Auger electron measurements have been reported above the C, O, and N K edges in a number of molecules.[16-17] The lack of anisotropy observed in these measurements[16,17] has been explained by the low-resolution experimental measurements which effectively sum over many individual Auger transitions, and by the possibly small values of c which would serve to reduce any substantial oscillation in a given ion orientation β_m.[16]

For the t_{2g} and "e_g" resonances in SF_6, the β for the $S(L_{2,3}VV)$ Auger peak was determined from the measured partial σ and β of the summed Auger and valence peaks, the measured total-valence cross section (Fig. 4), and assuming an unchanging total-valence β over the resonances. The estimated error is 10 percent in the total-valence cross section and ±0.10 for the total valence asymmetry

parameter. The resulting $S(L_{2,3}VV)$ Auger β, shown in Fig. 9, is not strongly affected by the resonances, within the experimental errors stated above. This result may be rationalized with the previous arguments that low-resolution measurements sum over individual Auger lines weighted by small values for c, smearing out effects in any one channel. Higher-resolution measurements will be valuable in testing this hypothesis. Meanwhile, the lack of a definite resonance effect on β_{Auger} is perplexing. If this observation is sustained by improved measurements, the lack of any significant anisotropy for β_{Auger} at the intense continuum resonances in SF_6 and other molecules would call for a reexamination of the predictions that a shape resonance should produce anisotropic emission of Auger electrons.

B. Discussion of the "e_g" Resonance

The most significant result at the "e_g" resonance is the enhancement of the satellite and main-line intensities at the same photon energy (Fig. 8). This behavior suggests that an excited quasibound or discrete SF_6 state is decaying to several (SF_6^+ + e^-) final states. In this section, we discuss and evaluate several possible interpretations of this behavior.

1. Conventional Models of Molecular Resonances

Currently, there are two well-understood and quite distinct types of molecular resonances: shape resonances (one-electron) and autoionization resonances.[10] As a start, each of these will be

examined as a possible interpretation for the "e_g" resonant decay.

First, if the 196.5 eV resonance is truly the e_g shape resonance, its decay into several channels is in conflict with the conventional one-electron picture of shape-resonance phenomena, which predicts decay into the main-line channel only. Because shape resonances have been described as final-state effects, in which a continuum electron is trapped by a potential barrier at a particular kinetic energy, we would expect to see satellite enhancement at the same kinetic energy as main-line enhancement,[55] rather than at the same photon energy. In other words, each satellite might show a shape resonance. The resonance kinetic energies would ordinarily be quite similar because the potential-field barriers would differ little from one satellite to another. In this simplest picture, each shape resonant event would proceed via a unique channel, through a particular barrier state to the corresponding final state in SF_6^+. Each channel would be resonant at its own characteristic kinetic energy. We must rule out this interpretation, based on our observation of main-line and satellite enhancement at the same photon energy.

Alternatively, an interpretation based on autoionizing states (doubly excited states of the neutral) could explain the decay to both main-line and satellite channels. Such a discrete state can couple to many final states. However, transitions to doubly excited states are typically an order of magnitude less intense than single excitations.[39] Furthermore, this explanation would require abandoning the well-established interpretation and supporting

theoretical work on the role of the e_g shape resonance in the S 2p continuum of SF_6. Even if we postulated that the 196.5 eV resonance were simply a doubly excited state, we would still have to account for the e_g shape resonance.

We prefer instead to combine the simple models for shape resonances and autoionizing states into a single, unified model which can be used to interpret our data by taking into account possible mixing of the two types of excited states through electron correlations. To set the stage for this more general approach, we briefly examine other atomic and molecular systems which exhibit unusual multielectron decay at shape resonances.

2. Observations on Other Systems

In atoms, a coupling of shape resonances to other channels has been observed in Xe and Ba.[56-60] For Xe, the 5p and 5s main-line photoemission cross sections are affected at the 4d$\rightarrow\varepsilon$f shape resonance.[56-57] However, Xe 4d photoemission still dominates the other channels by an order of magnitude.[56] In addition, measurements up to 75 eV photon energy suggest that some 5p and 5s correlation satellites are enhanced at the Xe 4d shape resonance.[58] For the 4d$\rightarrow$4,εf giant resonance in Ba just above the 4d threshold, preliminary reports indicate that 4d satellite intensities are influenced by the shape resonance, though the intensity maximum in the satellite cross sections may be offset in photon energy from the 4d main-line maximum.[60]

These examples illustrate the many-electron nature of the broad "collective" shape resonances in atoms. Similar interchannel interactions also may occur at molecular shape resonances. In fact, a similar coupling to nearby channels at $h\nu = 23$ eV has been seen in SF_6 for a feature interpreted as the valence t_{2g} shape resonance.[21-22] In N_2, some experimental[23-24] and theoretical[14] evidence indicates that continuum-continuum coupling could lead to an effect on β in the neighboring $2\sigma_u$ channel at about the photon energy of the $3\sigma_g \dashrightarrow \varepsilon\sigma_u$ shape resonance. However, these valence resonances in SF_6 and N_2 are not yet completely understood. For example, there may be possible complications in the SF_6 valence region due to autoionizing states.[21] Also, the K-matrix calculations for N_2 (Ref. 14) are preliminary at this point; there is a minimum in the $2\sigma_u$ experimental cross section,[61] but it is not clearly attributable to coupling with the $3\sigma_g \dashrightarrow \varepsilon\sigma_u$ shape resonance.

3. A Unified Model of Resonant Photoemission in SF_6

The SF_6 resonance behavior (t_{2g} in the valence shells,[21-22] and e_g in the S 2p level) may in fact be the first examples in which multi-electron effects are exhibited in molecular shape resonances. In addition to the resonant intensity behavior, the similarity of the β values for the S 2p main-line and the 189 eV satellite (Fig. 8) also supports this interpretation, which retains the qualitative aspects of a shape resonance while allowing for continuum-continuum coupling.

It is instructive to approach this problem by making a few observations about general principles that govern the electronic structure of molecules during dynamic processes, rather than trying to choose between oversimplified models such as one-electron shape resonances or double excitation. In this spirit, we observe that:

a. Any two (or more) states of the same symmetry, lying close in energy, would normally be expected to mix through electron correlation.

b. Mixing of these states will generally be reflected in an increased complexity of the resonant decay patterns, both in the relative intensities and numbers of final state channels.

c. When a shape resonance barrier is present, any discrete states lying close in energy to the continuum resonance will likely be strongly perturbed by it.

Within this general framework, there are several possible types of mixing. Firstly, the two degenerate channels may be in the continuum (S 2p main line and satellite in SF_6), leading to continuum-continuum coupling (also called interchannel coupling) as discussed previously. This mixing can be described as an additional complication to the expected one-electron behavior of the e_g shape resonance in S 2p ionization of SF_6. Secondly, there may be discrete doubly excited states of the neutral molecule which reside close in energy to the e_g shape resonance (the possibilities for these states will be elaborated on in the next section). These states couple to the continua through the discrete-continuum interactions described by Fano[62] as autoionization. Figure 10 illustrates the general aspects of this framework.

The extent to which each of these types of mixing affects the decay dynamics of the "e_g" resonance is not clear from the present experimental results. Rather, points a-c are meant to constitute a general, unified model of resonant photoemission. Of course, the degree of resonant enhancement in different channels will depend sensitively on the details of correlation mixing in each case.

The important consequence of this model is that it provides us with the insight that resonant photoemission in molecules need not be assigned strictly as a shape resonance or autoionization, but may in some cases be a perturbation on one model or a mixture of the two. This conclusion is a straightforward and inevitable consequence of the fact that electron correlation exists in excited molecular states. That electron correlation effects are sometimes readily observable is dramatically underscored by the data shown in Fig. 8.

In summary, the general model presented above includes continuum-continuum and discrete-continuum interactions, and can be used to rationalize enhancement of the 189 eV satellite at the "e_g" resonance. Clearly, calculations on SF_6 are needed to incorporate correlation effects at a practical level and focus the interpretation of the "e_g" resonance on the continuum interactions and importance of doubly excited states.

4. Further Spectroscopic Considerations on SF_6

We now examine in more detail the possibility of autoionization of doubly excited states in SF_6. If a doubly excited state is an important component of the resonant state near $h\nu = 196.5$ eV, then

there should be a corresponding satellite threshold at a higher photon energy. As mentioned earlier, we do observe a satellite with a binding energy of 205(2) eV, which is 7-11 eV above the "e_g" resonant feature, compared to the 8 eV energy separation of the S $2p \rightarrow 6a_{1g}$ discrete resonance and the S 2p threshold. Thus, the neutral doubly excited state and satellite configurations may be $SF_6(2p^{-1}v^{-1}6a_{1g}v^*)$ and $SF_6^+(2p^{-1}v^{-1}v^*)$ respectively, where v and v^* are, respectively, valence orbitals initially occupied or unoccupied in the ground state. The presence of an excited $6a_{1g}$ electron in the resonant-state configuration would help to explain the strong observed coupling to the 189(1) eV satellite, which we have proposed in Sec. IVA to have the configuration $SF_6^+[2p^{-1}(1t_{1g})^{-1}6a_{1g}]$.

We might also expect to see doubly excited resonances below the other observed satellite thresholds [189(1) and 194(1) eV]. For the 189(1) eV satellite, we believe that the most intense resonant states below this threshold would involve excitations into $6a_{1g}$ and $6t_{1u}$ molecular orbitals. One symmetry-allowed transition would lead to the configuration $2p^{-1}(1t_{1g})^{-1}6a_{1g}^2$, which would fall at about 186 eV (that is, 3 eV below the satellite threshold). The assigned t_{2g} shape resonance at 184 eV might include contributions from this configuration.

For the 194(1) eV satellite, by analogy with the above arguments, we would expect to see doubly excited resonances at 3 eV and 8 eV below this satellite threshold. The neutral resonant configurations would be $2p^{-1}v^{-1}v^*6t_{1u}$ (191 eV) and $2p^{-1}v^{-1}v^*6a_{1g}$ (186 eV), leading to the satellite configuration $2p^{-1}v^{-1}v^*$. While 186 eV photon energy

is a little higher than the resonance at 184 eV, there is no resonance evident at ~191 eV photon energy.

The above arguments for participation of doubly excited states in the sulfur L continuum spectrum are very tentative, for several reasons. First, our knowledge of molecular autoionization is very limited, especially with respect to doubly excited states. Secondly, the energies of the doubly excited states postulated above have been estimated using the energy spacing of the single excitations relative to the sulfur K and L shells of SF_6. This relative spacing will be different for a doubly excited state referenced to its corresponding satellite threshold, because of shifts arising from correlation and screening effects.

Several puzzling observations still remain. The "e_g" shape resonance not only produces an intense feature in the $L_{2,3}$ sub-shell cross section, but also exhibits strong multi-electron effects in its decay. By analogy, we would expect to see a similar feature in the valence-shell ionization channels of the proper symmetry (u). However, there is no evidence for even the existence of an outer-valence e_g shape resonance in SF_6. There is some evidence for an e_g resonance in the inner-valence levels of SF_6.[63]

The width of the "e_g" resonance in the L-shell (4 eV FWHM) is very narrow in comparison with shape resonances in other molecules at a comparable kinetic energy of ~15 eV. The existence of such a long-lived quasibound state at such high kinetic energy is experimentally unprecedented, and at odds with the resonance energy/width relationship obtained from the uncertainty principle for

quasibound states. For atoms, this energy/width relation has been parameterized by Connerade[64] with a shape-independent model, confirming that the resonances broaden out as the kinetic energy increases. MSM X-α calculations[49] which vary the N_2 bond distance over the range of the ground-state wave function also illustrate this trend in a given molecule. Of course, SF_6 has a very different molecular potential than atoms and diatomic molecules, so these comparisons may not strictly apply.

Still unassigned is the origin of the weak feature at $h\nu$ = 205 eV photon energy. Several possibilities exist. Excitation into doubly excited states of the neutral and/or into satellite continua of the ion have been proposed in the past to explain this broad feature in the total cross section.[4,6] Based on our tentative observation of some enhancement in the S 2p main-line channel in this energy region (see Fig. 7), we probably can rule out an explanation involving satellite continua onsets. We still allow for the contribution of doubly excited resonant states, though this interpretation seems problematic considering the energy proximity of the resonant feature (205 eV) with respect to the nearby satellite thresholds [205(2) eV]. Another proposal for this 205 eV feature involves the onset of "direct" ionization which occurs near this energy (just above the barrier associated with the e_g shape resonance).[3] As the electron kinetic energy exceeds the barrier height, a modulation in the cross section occurs.[3] To date, an observable cross-section effect of this nature is unprecedented, though it may occur in molecules (like SF_6) which exhibit unusually large continuum effects. Observation

of satellite enhancement near $h\nu$ = 205 eV would help to define the nature of this feature. Though we tentatively observe enhancement in the main line at this energy (see Fig. 7), low cross sections prohibited a similar measurement on the satellite peak.

V. Conclusions

The results reported here for photoionization near the S 2p edge in SF_6 have revealed the importance of many-electron effects at the unusually intense discrete and continuum resonances in the photon-energy range 160-260 eV. For the S $2p \rightarrow 6a_{1g}$ discrete transition, our low-resolution spectra yield qualitative information on the decay channels to SF_6^+. We observe valence-satellite enhancement predominantly in the binding-energy range of 30-80 eV, with several distinct peaks at 35 and 55 eV. We suspect that most of the satellites are "spectator" states, containing the initially excited $6a_{1g}$ electron. Some participatory decay was found, as evidenced by the small effect on the total outer-valence cross section. Because of overlap with satellites near 40 eV binding energy, we cannot rule out additional participatory decay to inner-valence main lines.

The specific assignment of the valence-satellite configurations enhanced at the $2p \rightarrow 6a_{1g}$ resonance has not been attempted because these peaks are very broad in our photoelectron spectrum and are probably associated with many configurations. Furthermore, interactions in the inner-valence orbitals of other molecules have

been found to require a many-body approach to model even the nonresonant main-line energies and intensities.[43] Higher resolution experiments might delineate this structure found in the binding-energy region 30-80 eV, while many-electron calculations for the inner-valence main lines and valence satellites would help to assign the individual peaks.

For the S 2p continuum resonances, our examination of the S 2p asymmetry parameter within 40 eV of threshold suggests that "atomic" sulfur behavior is embodied in the low kinetic-energy behavior. Comparison with other sulfur and silicon-containing molecules indicates that the 2p β's are surprisingly similar as a function of kinetic energy, despite the strong variations in the continuum resonance energies, widths, and intensities (See Fig. 1). In addition, the $S(L_{2,3}VV)$ Auger electron β remains near zero over both continuum resonances, contrary to qualitative theoretical predictions.[54] Despite the fact that the nature of the e_g resonance is uncertain, we believe that this lack of significant anisotropy at both continuum resonances in SF_6 and in other molecules may call for a reinvestigation into the relationship between molecular ion orientation and the angular characteristics of subsequent Auger electron emission.

In the S 2p continuum, the t_{2g} and e_g resonances in SF_6 have for years been used as illustrative and outstanding examples of how dramatically potential-barrier effects can modify the photoabsorption intensity near a core-level threshold. The enhancement of a S 2p correlation satellite at the assigned e_g

resonance throws serious doubt on the one-electron interpretation of this resonant feature (196.5 eV). It is noteworthy that a similar situation exists for the valence-shell ionization of SF_6, where several valence final states couple to a feature at 23 eV photon energy assigned as the t_{2g} shape resonance.[21-22]

We have proposed a heuristic unified model based on observation plus general features of many-electron systems to explain the S 2p satellite enhancement at the "e_g" resonance. Many-electron interactions, which are known to complicate the decay dynamics for atomic shape resonances, may play a role at the molecular shape resonances in SF_6. In a sense, the qualitative aspects of the shape resonance model still apply, with the decay properties modified by configuration-interaction in the continuum manifolds. The admixture of doubly excited states leading to S 2p satellite thresholds is also allowed for in this interpretation. Detailed theoretical calculations will be required to obtain a quantitative understanding of the origin of the unusual satellite enhancement at the e_g resonance, but we believe that the unified model described herein most likely provides the qualitative framework within which quantitative calculations can be performed. Finally, the nature of the broad cross-section feature at 205 eV photon energy is directly related to any consistent assignment of the e_g resonance. Thus, experiments on the decay properties of this broad peak could help to elucidate the role of many-electron and autoionization effects in this energy region.

Overall, these core-level photoemission results, along with recent experiments on the valence shells of SF_6,[21-22] present a major challenge to the understanding of molecular shape resonances. Rather than being a prototypical example of potential-barrier effects, SF_6 is most likely a very special case which provides us with a testing ground for investigating unusually strong many-electron interactions in molecules.

Acknowledgements

We would like to acknowledge helpful discussions with J.L. Dehmer, S.T. Manson, and T.D. Thomas. We thank S.T. Manson for performing the atomic calculations on β(S 2p). This work was supported by the Director, Office of Energy Research, Office of Basic Energy Sciences, Chemical Sciences Division of the U.S. Department of Energy under Contract No. DE-AC03-76SF00098. It was performed at the Stanford Synchrotron Radiation Laboratory, which is supported by the Department of Energy's Office of Basic Energy Sciences. One of the authors (M.N.P.) was a Fulbright Scholar during this project.

References

1. T.M. Zimkina and V.A. Formichev, Sov. Phys. Dokl. 11, 726 (1967).
2. T.M. Zimkina and A.S. Vinogradov, J. Phys. (Paris) 32, C4-3 (1971).
3. J.L. Dehmer, J. Chem. Phys. 56, 4496 (1972) and references therein.
4. F.A. Gianturco, C. Guidotti, and U. Lamanna, J. Chem. Phys. 57, 840 (1972).
5. R.E. LaVilla, J. Chem. Phys. 57, 899 (1972).
6. A.P. Hitchcock and C.E. Brion, Chem. Phys. 33, 55 (1978).
7. A.P. Hitchcock, C.E. Brion, and W.J. Van der Wiel, J. Phys. B 11, 3245 (1978).
8. R.S. Wallace, Ph.D. thesis, Boston University, 1980.
9. E. Ishiguro, K. Soda, A. Mikuni, Y. Suzuki, S. Iwata, and T. Sasaki, SOR-RING Activity Report, 66 (1982).
10. J.L. Dehmer, D. Dill, and A.C. Parr in Photophysics and Photochemistry in the Vacuum Ultraviolet, edited by S.P. McGlynn, G. Findley, and R. Huebner (Riedel, Dordrecht, Holland, 1985) p. 341.
11. J.L. Dehmer and D. Dill in Electron-Molecule and Photon-Molecule Collisions, edited by T. Rescigno, V. McKoy, and B. Schneider (Plenum Press, New York, 1979) p. 225 and references therein.
12. P.W. Langhoff in Electron-Molecule and Photon-Molecule Collisions, edited by T. Rescigno, V. McKoy, and B. Schneider (Plenum Press, New York, 1979) p. 183.

13. V. McKoy, T.A. Carlson, and R.R. Lucchese, J. Chem. Phys. 88, 3188 (1984); D.L. Lynch, V. McKoy, and R.R. Lucchese in Resonances in Electron-Molecule Scattering, van der Waals Complexes, and Reactive Chemical Dynamics, edited by D.G. Truhlar (American Chemical Society, Washington, D.C., 1984).

14. J.A. Stephens and D. Dill, Phys. Rev. A 31, 1968 (1985); B. Basden and R.R. Lucchese, Phys. Rev. A 37, 89 (1988).

15. See for example G.R. Wight, C.E. Brion, and M.J. Van der Wiel, J. Electron Spectrosc. 1, 457 (1972/73); G.R. Wight and C.E. Brion, 3, 191 (1974); 4, 313 (1974); 4, 327 (1974); A.P. Hitchcock and C.E. Brion, 10, 317 (1977); A. Bianconi, H. Peterson, F.C. Brown, and R.Z. Bachrach, Phys. Rev. A 17, 1907 (1978); R.N.S. Sodhi, S. Daviel, C.E. Brion, and G.G.B. De Souza, J. Electron Spectrosc. 35, 45 (1985).

16. C.M. Truesdale, D.W. Lindle, P.H. Kobrin, U.E. Becker, H.G. Kerkhoff, P.A. Heimann, T.A. Ferrett, and D.A. Shirley, J. Chem. Phys. 80, 2319 (1984).

17. D.W. Lindle, C.M. Truesdale, P.H. Kobrin, T.A. Ferrett, P.H. Heimann, U. Becker, H.G. Kerkhoff, and D.A. Shirley, J. Chem. Phys. 81, 5375 (1984).

18. T.A. Carlson, W.A. Svensson, M.O. Krause, T.A. Whitley, F.A. Grimm, G.V. Wald, J.W. Taylor, and B.P. Pullen, J. Chem. Phys. 84, 122 (1986).

19. G.M. Bancroft, S. Aksela, H. Aksela, K.H. Tan, B.W. Yates, L.L. Coatsworth, and J.S. Tse, J. Chem. Phys. 84, 5 (1986); S. Aksela, K. H. Tan, H. Aksela, and G. M. Bancroft, Phys. Rev. A 33, 258 (1986); T.A. Ferrett, M.N. Piancastelli, D.W. Lindle, P.A. Heimann, and D.A. Shirley, Phys. Rev. A (in press).

20. G.G.B. de Souza, P. Morin, and I. Nenner, J. Chem. Phys. 83, 492 (1985); P. Morin, G.G.B. de Souza, and I. Nenner, Phys. Rev. Lett. 56, 131 (1986).

21. J.L. Dehmer, A.C. Parr, S. Wallace, and D. Dill, Phys. Rev. A 26, 3283 (1982).

22. T. Gustafsson, Phys. Rev. A 18, 1481 (1978).

23. G.V. Marr, J.M. Morton, R.M. Holmes, and D.G. McKoy, J. Phys. B 12, 43 (1979).

24. S. Southworth, A.C. Parr, J.E. Hardis, and J.L. Dehmer, Phys. Rev. A 33, 1020 (1986).

25. D. Loomba, S. Wallace, D. Dill, and J.L. Dehmer, J. Chem. Phys. 75, 4546 (1981).

26. M.G. White, R.A. Rosenberg, G. Gabor, E.D. Poliakoff, G. Thornton, S. Southworth, and D.A. Shirley, Rev. Sci. Instrum. 50, 1288 (1979).

27. S. Southworth, C.M. Truesdale, P.H. Kobrin, D.W. Lindle, W.D. Brewer, and D.A. Shirley, J. Chem. Phys. 76, 143 (1982).

28. S. Southworth, U. Becker, C.M. Truesdale, P.H. Kobrin, D.W. Lindle, S. Owaki, and D.A. Shirley, Phys. Rev. A 28, 261 (1983).

29. C.N. Yang, Phys. Rev. 74, 764 (1948).

30. F. Wuilleumier and M.O Krause, J. Electron Spectrosc. 15, 15 (1979).

31. T.A. Carlson, M.O Krause, F.A. Grimm, P.R. Keller, and J.W. Taylor, Chem. Phys. Lett. 87, 552 (1982); D.W. Lindle, P.A. Heimann, T.A. Ferrett, P.H. Kobrin, C.M. Truesdale, U. Becker, H.G. Kerkhoff, and D.A. Shirley, Phys. Rev. A 33, 319 (1986).

32. D.W. Lindle, T.A. Ferrett, P.A. Heimann, and D.A. Shirley, Phys. Rev. A 34, 1131 (1986).

33. K. Siegbahn, C. Nordling, G. Johansson, J. Hedman, P.F. Heden, K. Hamrin, U. Gelius, T. Bergmark, L.O. Werme, R. Manne, and Y. Baer, ESCA Applied to Free Molecules (North-Holland, Amsterdam, 1969).

34. L. Ungier and T.D. Thomas, Chem. Phys. Lett. 96, 247 (1983).

35. C.M. Truesdale, S.H. Southworth, P.H. Kobrin, U. Becker, D.W. Lindle, H.G. Kerkhoff, and D.A. Shirley, Phys. Rev. Lett. 50, 1265 (1983).

36. H.W. Haak, G.A. Sawatzky, L. Ungier, J.K. Gimzewski, and T.D. Thomas, Rev. Sci. Instrum. 55, 696 (1984).

37. L. Ungier and T.D. Thomas, J. Chem. Phys. 82, 3146 (1985).

38. U. Becker, R. Holzel, H.G. Kerkhoff, B. Langer, D. Szostak, and R. Wehlitz, Phys. Rev. Lett. 56, 1455 (1986).

39. T.A. Ferrett, D.W. Lindle, P.A. Heimann, H.G. Kerkhoff, U.E. Becker, and D.A. Shirley, Phys. Rev. A 34, 1916 (1986).

40. For convenience, we choose to differentiate between inner-valence main lines and satellites in this energy range even though some of these states may be nearly degenerate in energy, requiring a many-body approach to assigning configurations. The role of many-body aspects in the SF_6 valence region should emerge as both higher resolution experiments and calculations are performed.

41. S. Anderson and T.D. Thomas (private communication).

42. The integration for this "inner"-valence region includes a tail extending to ~100 eV binding energy. Part of this tail may be caused by shake-off processes which could be enhanced at the resonance. Nonetheless, most of the integrated intensity in this energy region is associated with the production of singly-charged ions.

43. L.S. Cederbaum, W. Domcke, J. Schirmer, and W. von Niessen, Adv. Chem. Phys. 65, 115 (1986).

44. N. Martensson, P.A. Malmquist, S. Svensson, E. Basilier, J.J. Pireaux, U. Gelius, and K. Siegbahn, Nouv. J. de Chim. 1, 191 (1977); H. Ågren and H. Siegbahn, Chem. Phys. Lett. 69, 424 (1980); M. Mishra and Y. Ohrn, Chem. Phys. Lett. 71, 549 (1980); R. Arneberg, J. Muller, and R. Manne, Chem. Phys. 64, 249 (1982); H. Nakatsuji and T. Yonezawa, Chem. Phys. Lett. 87, 426 (1982); W. von Niessen, L.S. Cederbaum, J. Schirmer, G. Diercksen, and W.P. Kramer, J. Electron Spectrosc. 28, 45 (1982); R. Cambi, G. Ciullo, A. Sgamellotti, C.E. Brion, J.P.D. Cook, I.E. McCarthy, and E. Weigold, Chem Phys. 91, 373 (1984); 98, 166 (1985); C.E. Brion, D.W. Lindle, P.A. Heimann, T.A. Ferrett, and M.N. Piancastelli, Chem. Phys. Lett. 128, 118 (1986).

45. W. Domcke, L.S. Cederbaum, J. Schirmer, W. von Niessen, and J.P. Maier, J. Electron Spectrosc. 14, 59 (1978); C.E. Brion, J.P.D. Cook, and K.H. Tan, Chem. Phys. Lett. 59, 241 (1978); J.P.D. Cook, C.E. Brion, and A. Hamnett, Chem. Phys. 45, 1 (1980); M.Y. Adam, P. Morin, C. Cauletti, and M.N. Piancastelli, J. Electron Spectrosc. 36, 377 (1985).

46. P.R. Keller, J.W. Taylor, F.A. Grimm, P. Senn, T.A. Carlson, and M.O. Krause, Chem. Phys. 74, 247 (1983).

47. S.T. Manson (private communication); S.T. Manson, J. Electron Spectrosc. 1, 413 (1972/73).

48. W. von Niessen, L.S. Cederbaum, G.H.F. Diercksen, and G. Hohlneicher, Chem. Phys. 11, 399 (1975); P.J. Hay, J. Am. Chem. Soc. 99, 1013 (1977); W. von Niessen, W.P. Kraemer, and G.H.F. Diercksen, Chem. Phys. Lett. 63, 65 (1979).

49. J.L. Dehmer, D. Dill, and S. Wallace, Phys. Rev. Lett. 43, 1005 (1979).

50. D.L. Lynch and V. McKoy, Phys. Rev. A 30, 1561 (1984).

51. Z.H. Levine and P. Soven, Phys. Rev. A 29, 625 (1984).

52. D. Dill, S. Wallace, J. Siegel, and J.L. Dehmer, Phys. Rev. Lett. 42, 411 (1979); F.A. Grimm, Chem. Phys. 53, 71 (1980); R.R. Lucchese and B.V. McKoy, Phys. Rev. A 26, 1406 (1982).

53. H. Friedrich, B. Pittel, P. Rabe, W.H.E. Schwarz, and B. Sonntag, J. Phys. B 13, 25 (1980); A.S. Vinogradov and T.M. Zimkina, Opt. Spectrosc. 31, 288 (1971).

54. D. Dill, J.S. Swanson, S. Wallace, and J.L Dehmer, Phys. Rev. Lett. 45, 1393 (1980); S. Wallace and D. Dill, Phys. Rev. B 17, 1692 (1978).

55. There should be small differences in the resonant kinetic energy for main lines and satellites caused by the interaction with the different residual ions. In order to explain the satellite enhancement at 196.5 eV in SF_6, this difference would have to be about 8 eV and coincidentally equal to the satellite excitation energy.

56. J.B. West, P.R. Woodruff, K. Codling, and R.G. Houlgate, J. Phys. B 9, 407 (1976).

57. M. Ya. Amusia and U.K. Ivanov, Phys. Lett. 59A, 194 (1976); L. Torop, J. Morton, and J.B. West, J. Phys. B 9, 2035 (1976); U. Becker, T.-Prescher, E. Schmidt, B. Sonntag, and H.-E. Wetzel, Phys. Rev. A 33, 3891 (1986).

58. A. Fahlman, M.O. Krause, T.A. Carlson, and A. Svensson, Phys. Rev. A 30, 812 (1984).

59. M.H. Hecht and I. Lindau, Phys. Rev. Lett. 47, 821 (1981).

60. U. Becker, R. Holzel, H.G. Kerkhoff, B. Langer, D. Szostak, and R. Wehlitz, ICPEAC Abstracts, Palo Alto, CA, July 1985.

61. A. Hamnett, W. Stoll, and C.E. Brion, J. Electron Spectrosc. 8, 367 (1976).

62. U. Fano, Phys. Rev. 124, 1866 (1961).

63. T.A. Ferrett, M.N. Piancastelli, P.A. Heimann, L.J. Medhurst, S.H. Liu, and D.A. Shirley, Chem. Phys. Lett. 143, 146 (1987).

64. J.P. Connerade, J. Phys. B 17, L165 (1984).

Figure Captions

Fig. 1 Photoabsorption spectra of SF_6 (Ref. 1), SiF_4 (Ref. 53), and SO_2 (Ref. 2) plotted on arbitrary cross-section scales for qualitative comparison. The spectra have been lined up in kinetic energy relative to the S or Si 2p edges in these molecules.

Fig. 2 Molecular-orbital diagram for SF_6. The energy levels are not drawn to scale. The order of the valence shells is taken from Ref. 21. Excitation of a S 2p electron to the discrete $6a_{1g}$ level is shown, as are transitions to the t_{2g} and "e_g" continuum shape resonances.

Fig. 3 TOF spectrum at 196.4 eV photon energy and θ=54.7°, taken at the peak of the "e_g" resonance. The binding energy of the enhanced S 2p correlation satellite is 189(1) eV.

Fig. 4 Total photoabsorption cross section[1] for SF_6. The present total yield data (solid circles) from the sum of the $S(L_{2,3}VV)$ Auger- and valence-electron intensity in SF_6 has been scaled to the photoabsorption curve at 189.3 eV. The dashed curve represents an estimate of the valence main-line cross section (both inner- and outer-valence) above the S 2p threshold, based on the valence intensity in the TOF spectra over this energy range.

Fig. 5 Binding-energy spectra taken off (176.1 eV) and on (172.9 eV) the S 2p$\longrightarrow 6a_{1g}$ discrete resonance. The peaks labelled outer valence consist of the unresolved $1t_{1g}$, $1t_{2u}$, $5t_{1u}$, $3e_g$, $1t_{2g}$, $4t_{1u}$, and $5a_{1g}$ orbitals. The region labelled "inner" valence includes the inner-valence main lines ($2e_g$, $3t_{1u}$, and $4a_{1g}$) and all valence satellites between 30 and 100 eV binding energy.

Fig. 6 Relative partial cross sections for the outer- and "inner"-valence peaks near the S 2p$\longrightarrow 6a_{1g}$ discrete excitation (top). The "inner"-valence cross section represents the binding-energy range of 30-100 eV in the TOF spectra. The corresponding "inner"-valence β is shown also (bottom).

Fig. 7 S 2p asymmetry parameter (top) and partial cross section (bottom) for SF_6 (solid circles). MSM-Xα results[8] for β are shown, with the theory curve shifted to the experimental "e_g" resonance energy. The atomic β(2p) for sulfur is also plotted.[47] The open circles for β are the measured Si 2p values for SiF_4 (Ref. 46) plotted as a function of kinetic energy for ease of comparison.

Fig. 8 Relative cross section and asymmetry parameter for the S 2p main line (solid circles) and satellite (open circles) in an expanded energy range near the "e_g" resonance (196.5 eV).

Fig. 9 Asymmetry parameter for the sulfur $L_{2,3}VV$ Auger electrons in the vicinity of the t_{2g} (184 eV) and e_g (196.5 eV) resonances. Arrows mark the resonance positions observed in the cross section.

Fig.10 An energy-level diagram depicting the resonant state (Ψ_{RES}) at E_{RES} = 196.5 eV relative to the ground state (g.s.), and its coupling to both the S 2p main-line (ML) and satellite (SAT) continua. Electron correlation allows the e_g resonance to couple to both the main-line and satellite continua, and to doubly excited states of the neutral molecule. The resonant state Ψ_{RES} is drawn to illustrate this mixed discrete-continuum character.

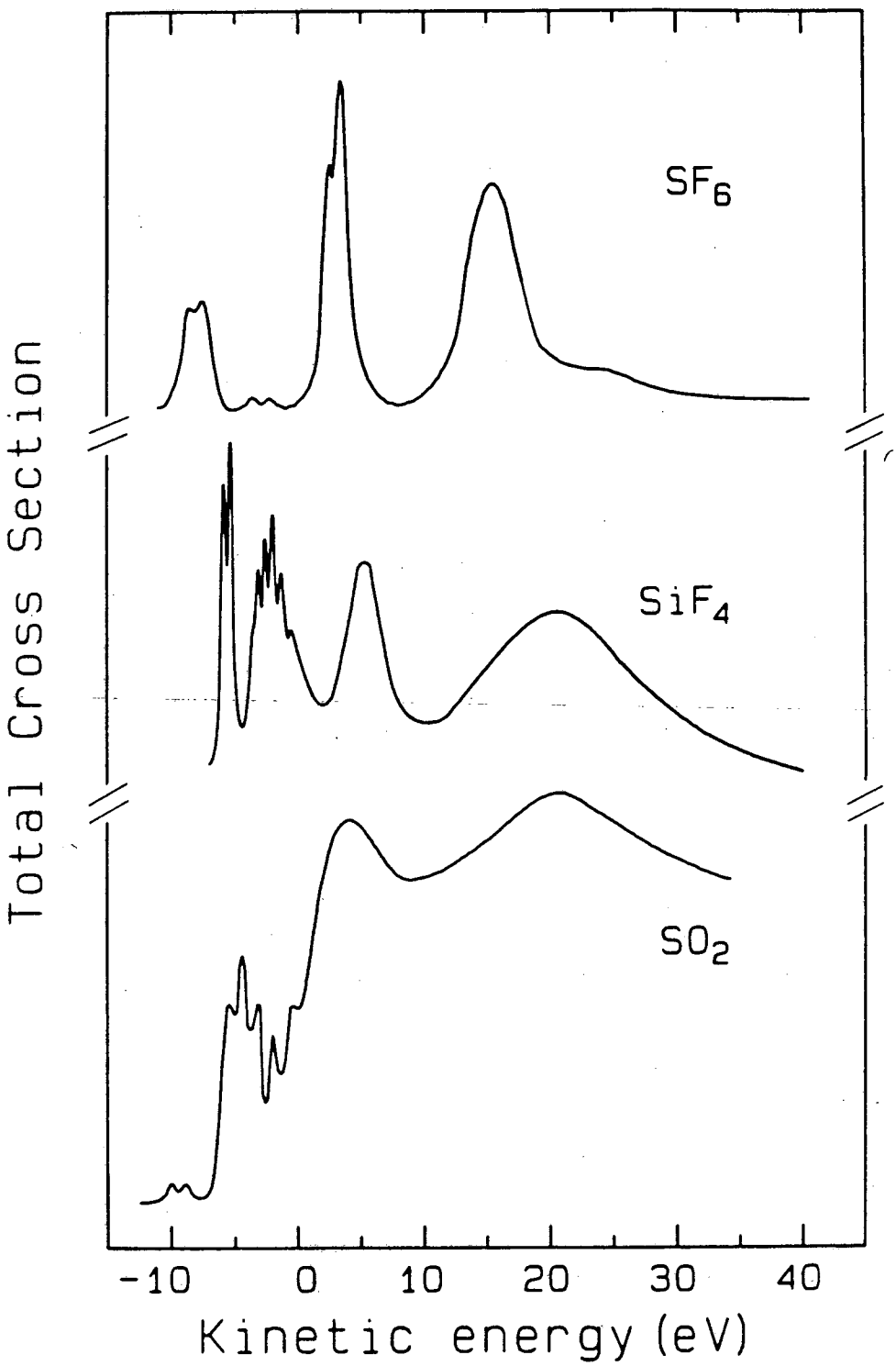

XBL 8611-4299

Figure 1

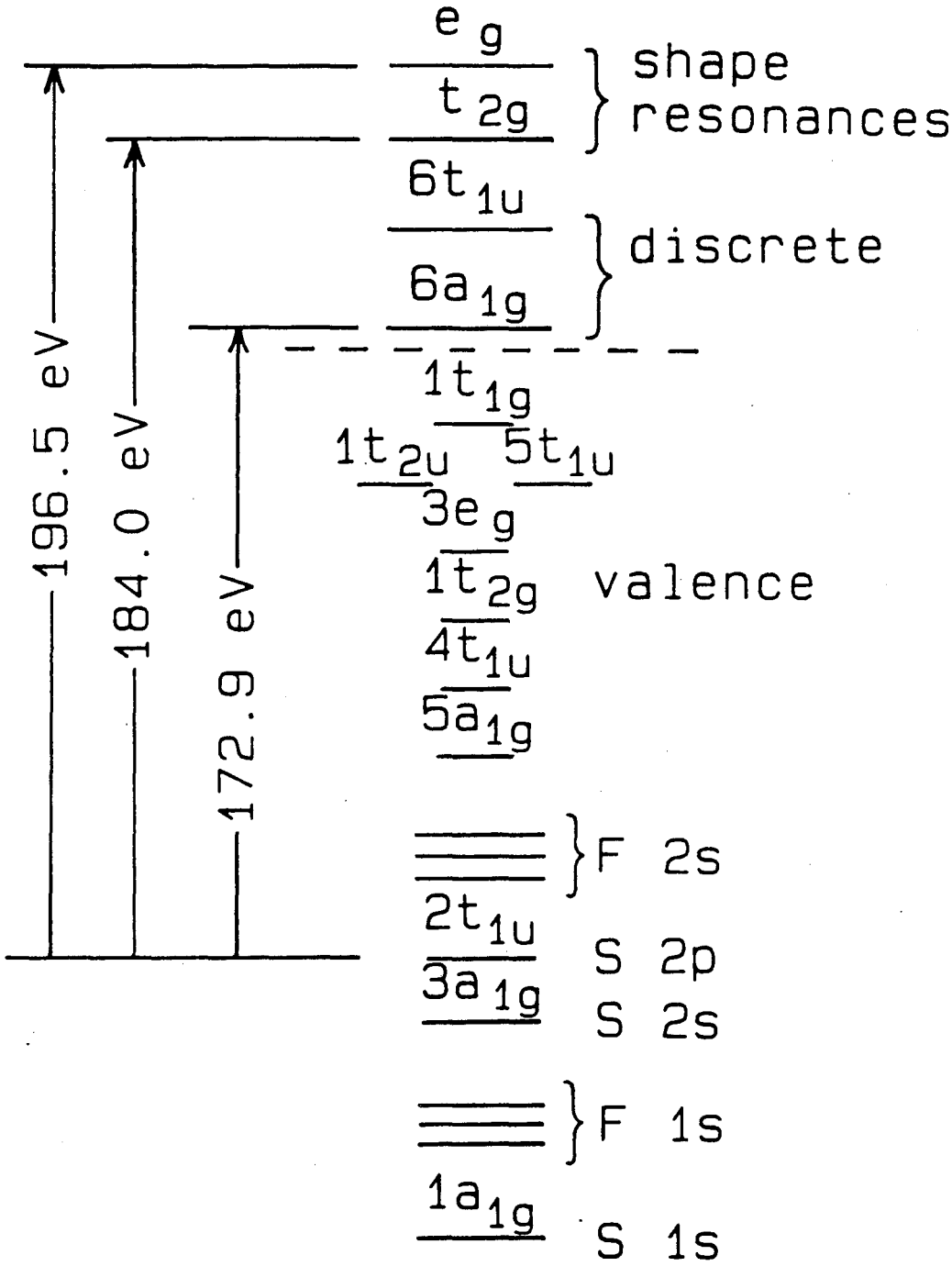

XBL 8611-4300

Figure 2

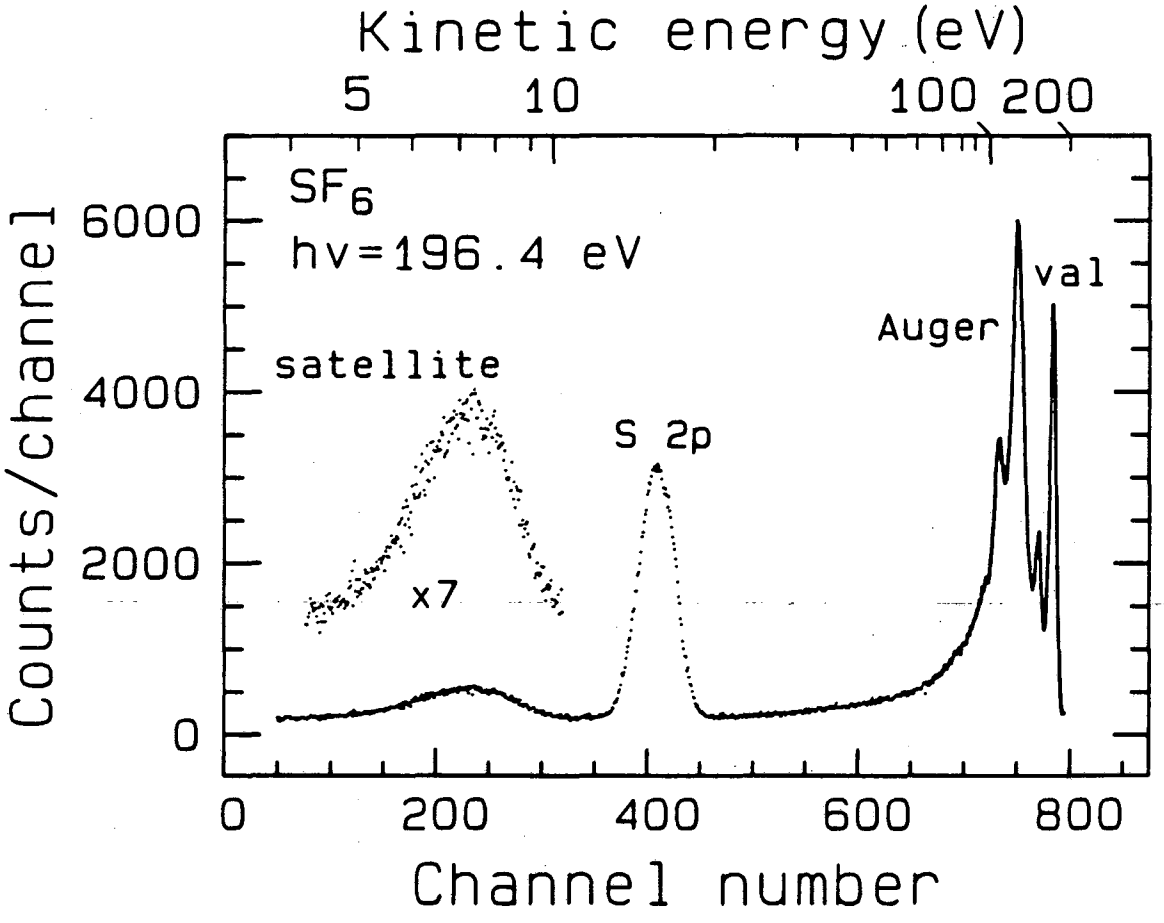

XBL 8611-4298

Figure 3

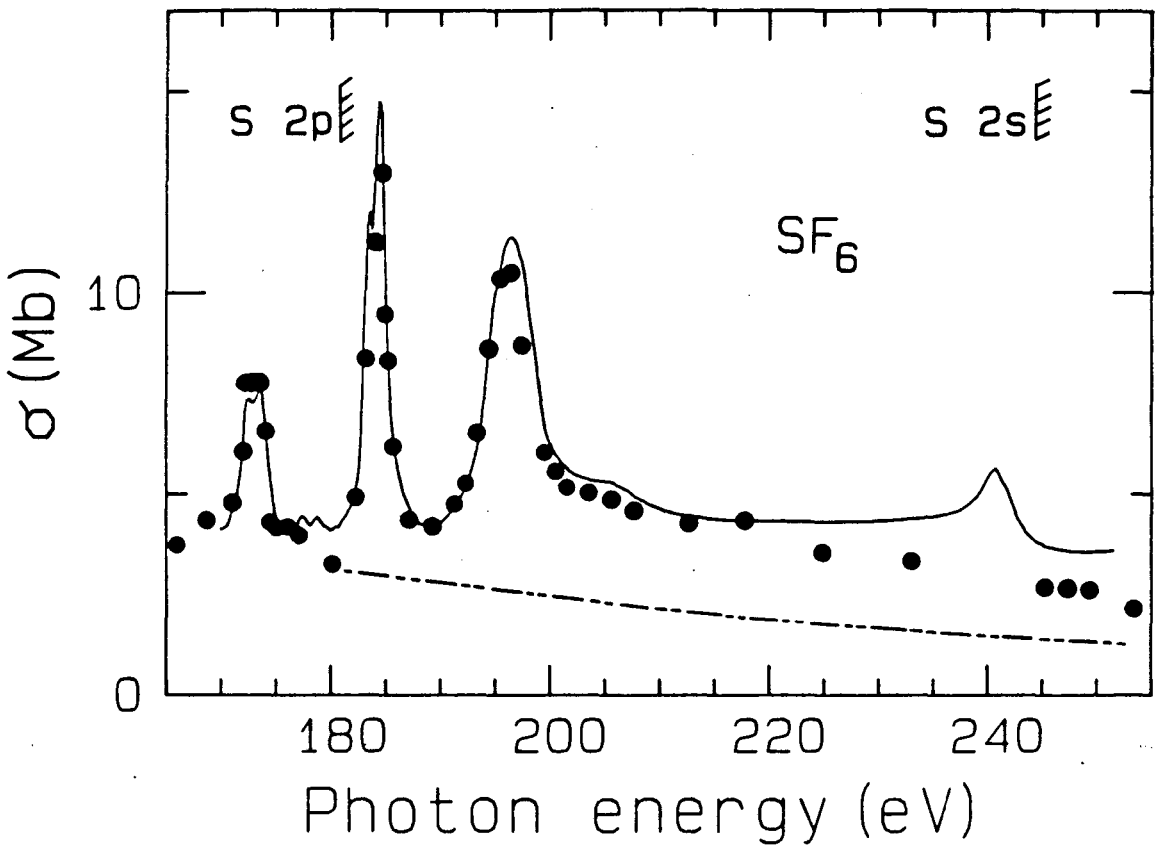

XBL 8611-4297

Figure 4

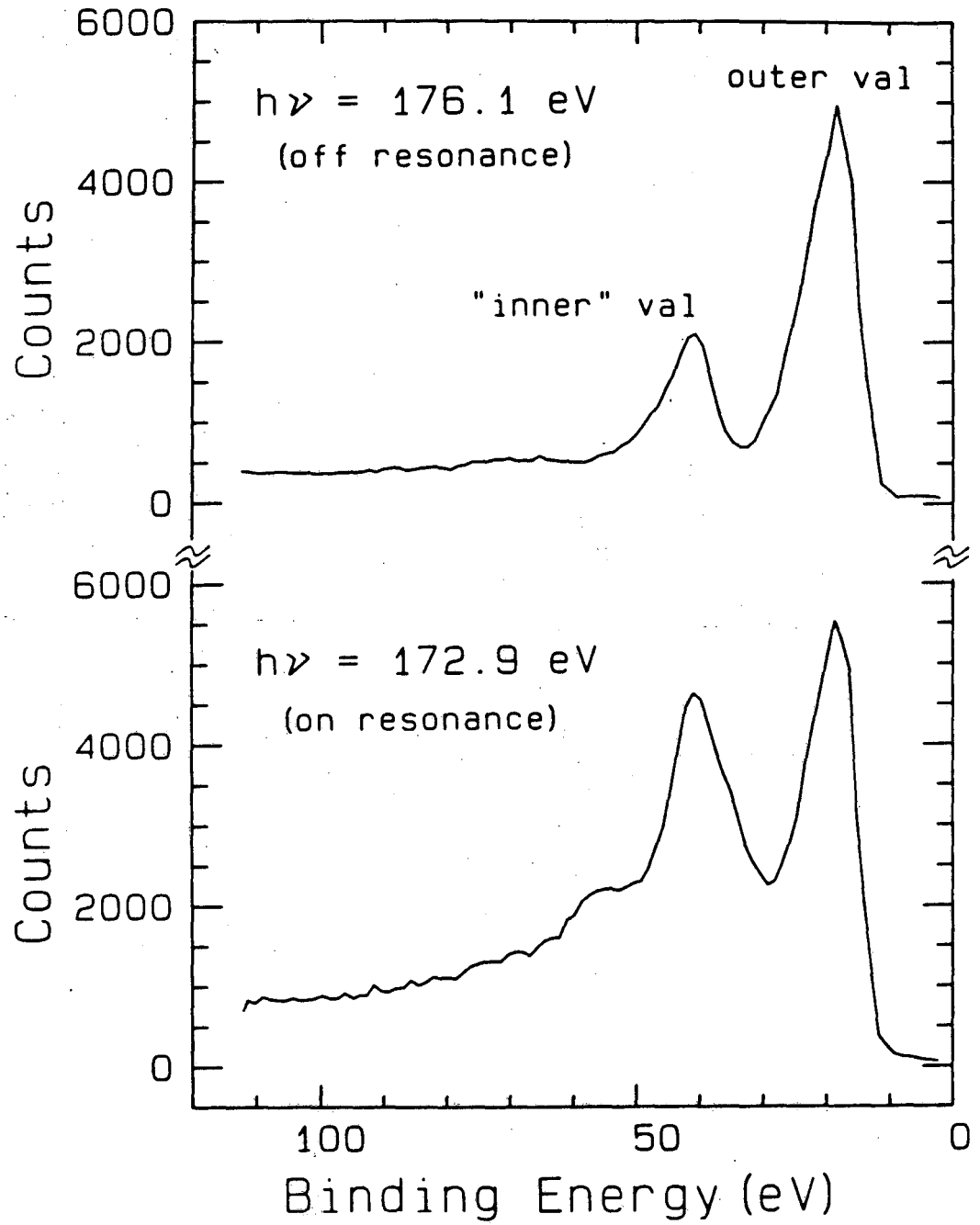

Figure 5

XBL 8611-4296

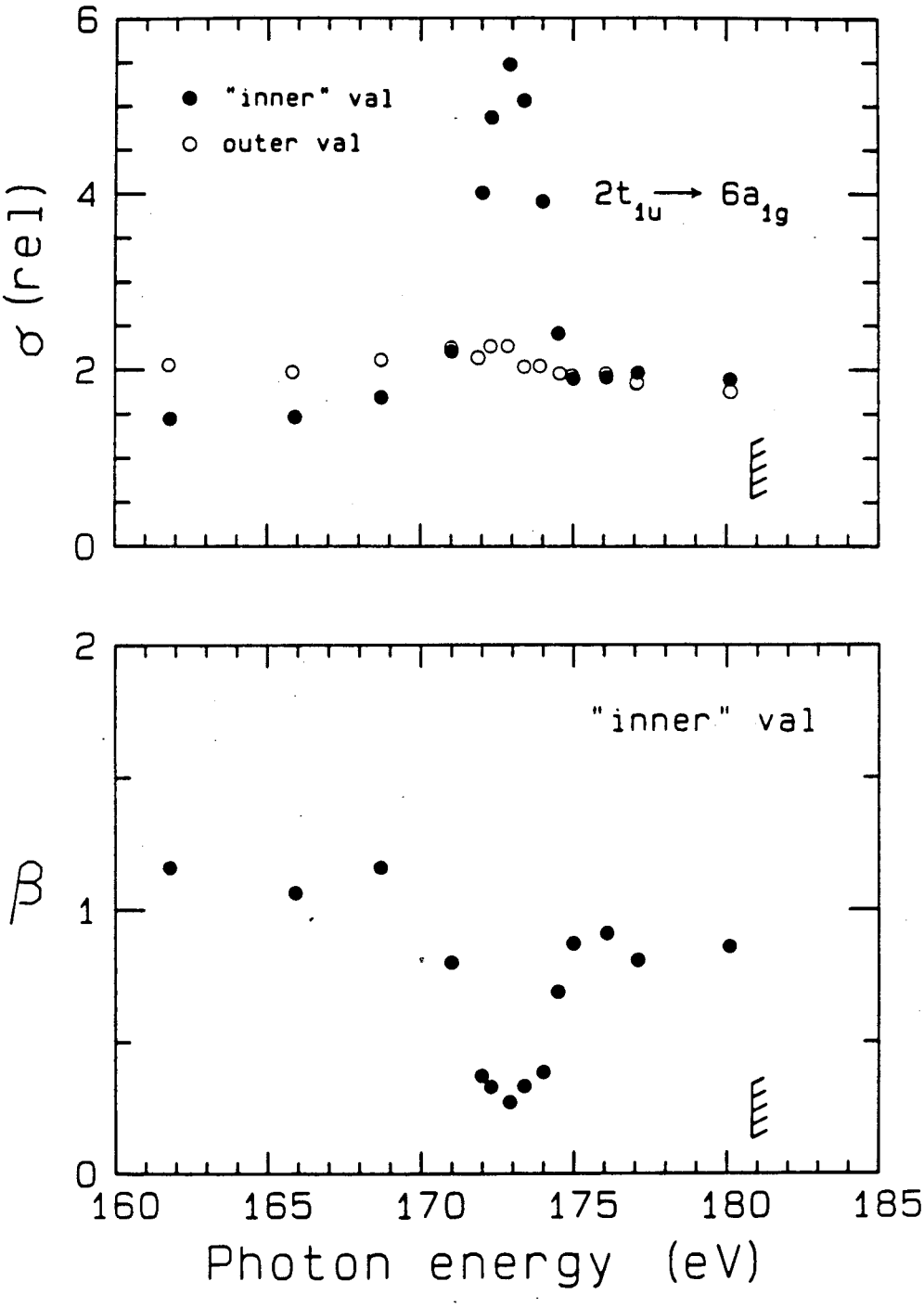

Figure 6

XBL 8611-4295

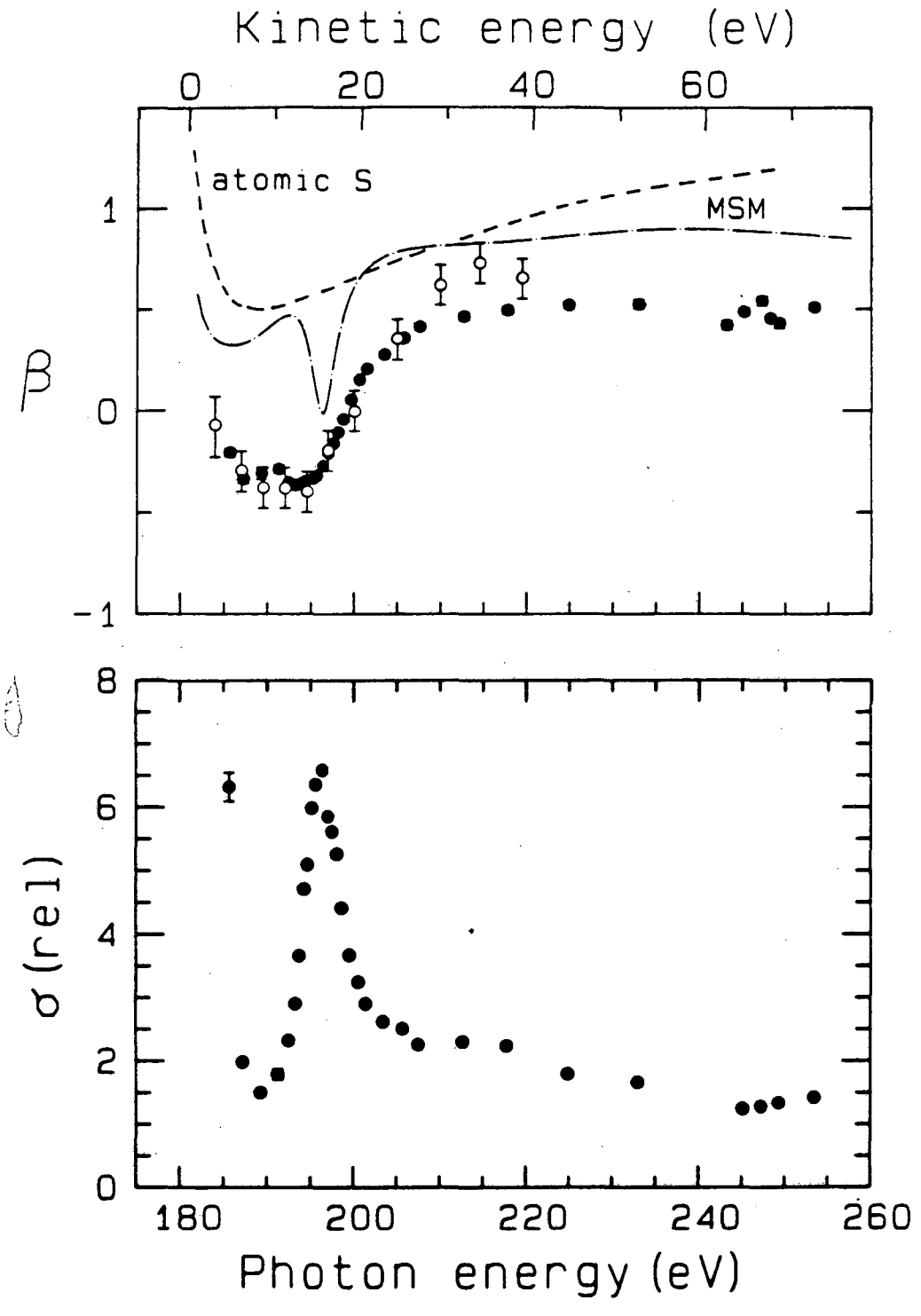
Kinetic energy (eV)
0
20
40
60
atomic S
MSM
1
0
-1
β
8
6
4
2
0
σ(rel)
180
200
220
240
260
Photon energy (eV)
XBL 8611-4573

Figure 7

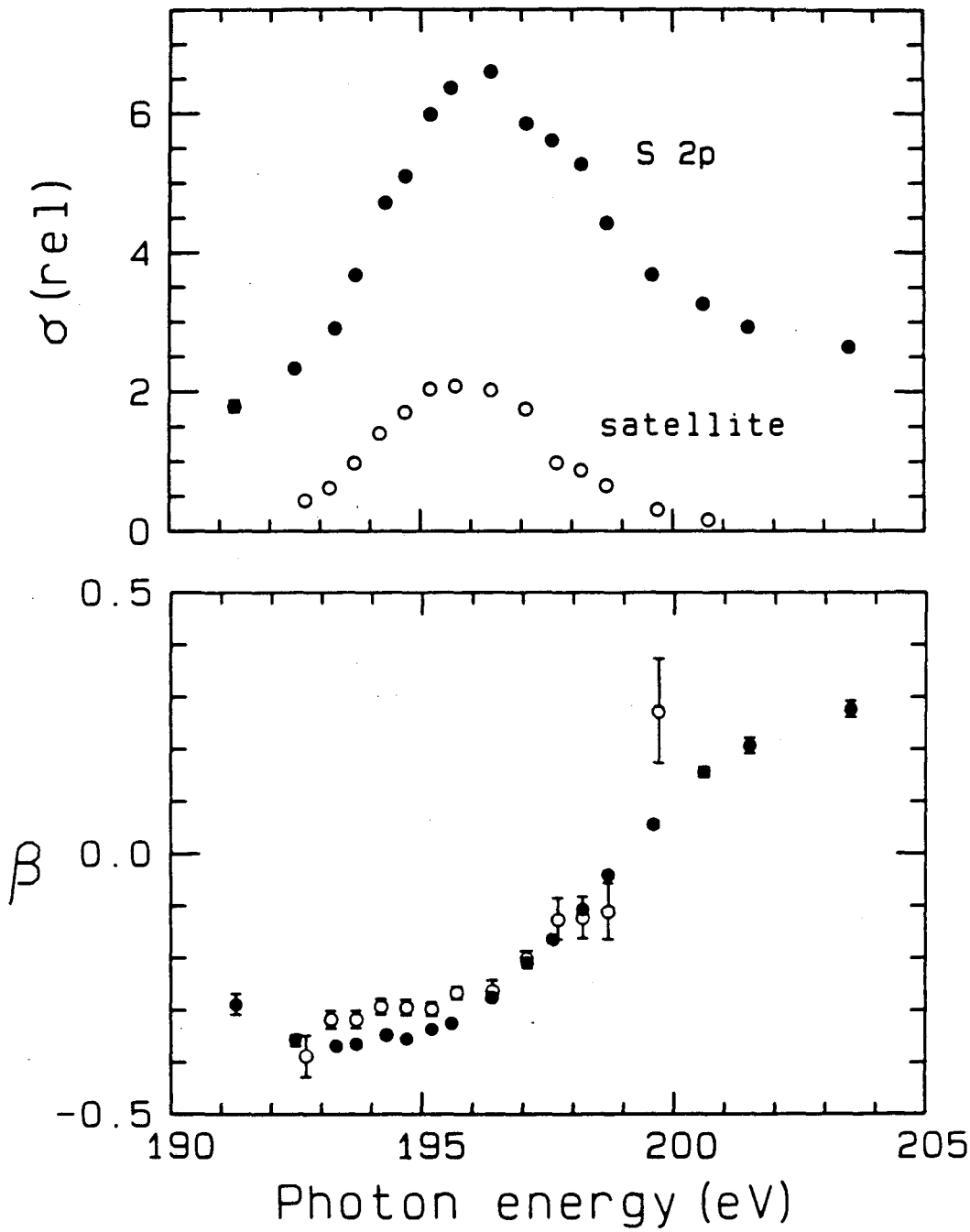

Figure 8

XBL 8611-4293

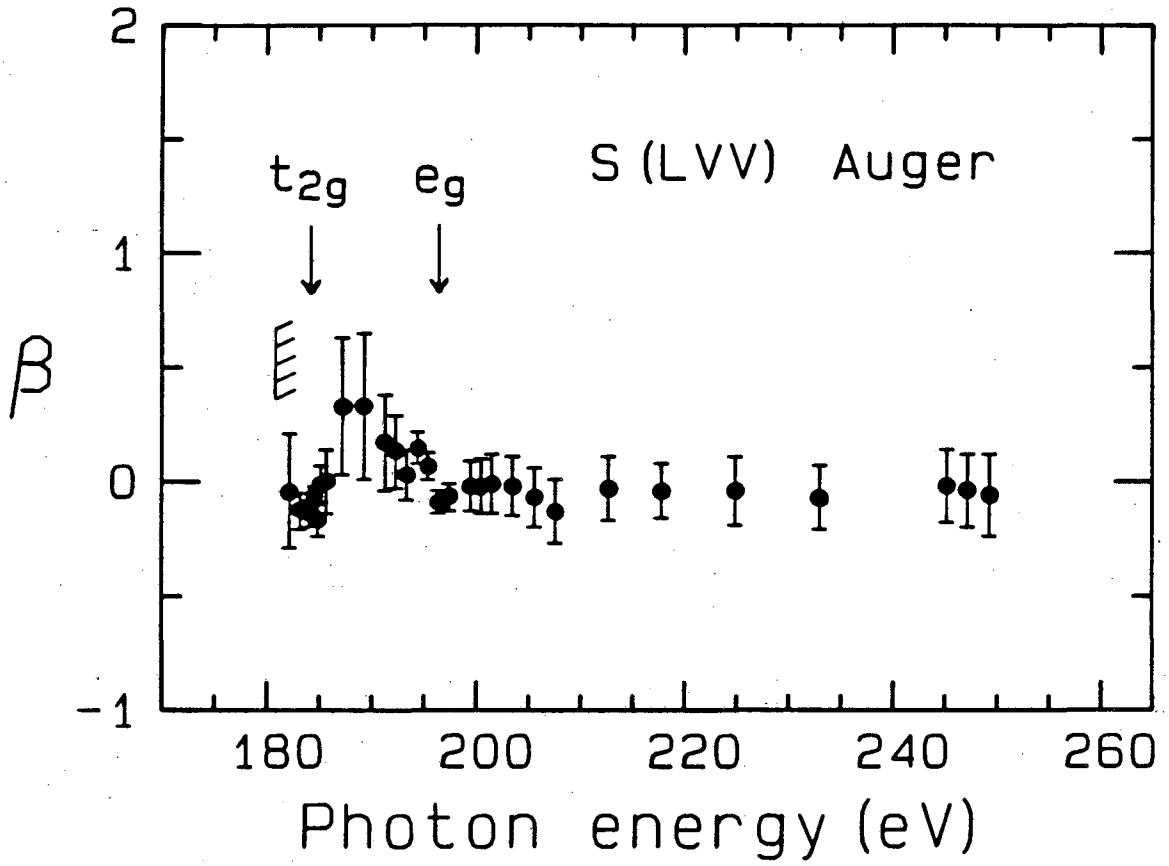

XBL 8611-4292

Figure 9

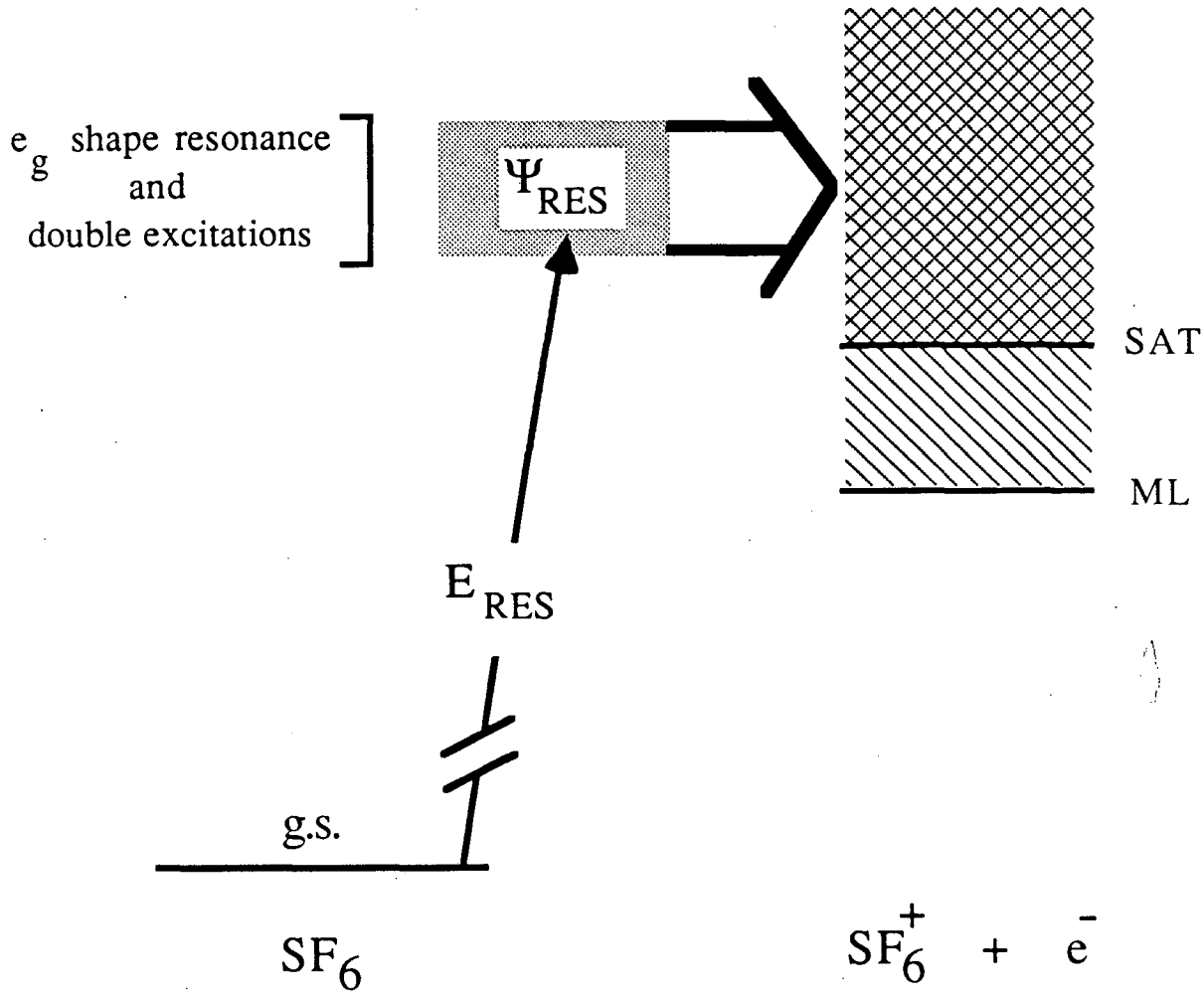

XBL 884-1088

Figure 10

LAWRENCE BERKELEY LABORATORY
TECHNICAL INFORMATION DEPARTMENT
UNIVERSITY OF CALIFORNIA
BERKELEY, CALIFORNIA 94720